Biochemical and Biophysical Research Communications **290,** 311–317 (2002)
doi:10.1006/bbrc.2001.6142, available online at http://www.idealibrary.com on IDEAL®

Class VI Myosin Moves Processively along Actin Filaments Backward with Large Steps

So Nishikawa,*,† Kazuaki Homma,‡ Yasunori Komori,† Mitsuhiro Iwaki,§ Tetsuichi Wazawa,* Atsuko Hikikoshi Iwane,§ Junya Saito,‡ Reiko Ikebe,‡ Eisaku Katayama,¶,‖ Toshio Yanagida,*,†,§,[1] and Mitsuo Ikebe‡,[1]

**Single Molecule Process Project, ICORP, JST, 2-4-14, Senba-Higashi, Mino, Osaka 562-0035, Japan; †Department of Biophysical Engineering, Osaka University, 1-3, Machikaneyama, Toyonaka, Osaka 560-8531, Japan; ‡Department of Physiology, University of Massachusetts Medical School, 55 Lake Avenue North, Worcester, Massachusetts 01655-0127; §Department of Physiology and Biosignaling, Graduate School of Medicine, Osaka University, 2-2, Yamadaoka, Suita, Osaka 565-0871, Japan; ¶Division of Biomolecular Imaging, Institute of Medical Science, University of Tokyo, Minato-ku, Tokyo, 108-8639, Japan; and ‖PRESTO, JST, Kawaguchi, Saitama 332-0012, Japan*

Received November 20, 2001

Among a superfamily of myosin, class VI myosin moves actin filaments backwards. Here we show that myosin VI moves processively on actin filaments backwards with large (~36 nm) steps, nevertheless it has an extremely short neck domain. Myosin V also moves processively with large (~36 nm) steps and it is believed that myosin V strides along the actin helical repeat with its elongated neck domain that is critical for its processive movement with large steps. Myosin VI having a short neck cannot take this scenario. We found by electron microscopy that myosin VI cooperatively binds to an actin filament at ~36 nm intervals in the presence of ATP, raising a hypothesis that the binding of myosin VI evokes "hot spots" on actin filaments that attract myosin heads. Myosin VI may step on these "hot spots" on actin filaments in every helical pitch, thus producing processive movement with 36 nm steps.

Key Words: **myosin VI; actin; GFP; optical trap; single molecule imaging; Brownian motion; vesicle transport; molecular motor; nanotechnology.**

MyosinVI is composed of two heavy chains, each consisting of a motor domain, one IQ motif that binds a calmodulin light chain (neck domain), an α-helical coiled–coil, and a small globular C-terminal domain that is thought to play a critical role in determining the specificity of each myosin in cellular environment by interacting with the isoform specific targets (Fig. 1A, left) (1). A number of studies support the idea that myosin VI plays a role in organelle transport as well as other functions such as the reorganization of actin filaments and microtubules (2–5). A most striking finding is that among a superfamily of at least 18 known classes of myosin, myosin VI moves actin filaments in the backward direction (6). This raised the possibility that intracellular organelles can move on actin filaments in both directions. The "processivity" of the motors is critical to support cargo movement and several evidences now indicate that myosin V is a processive motor that supports cargo movement on actin cables to the plus direction (7–9). A key question is whether myosin VI is "processive" and thus supports the cargo movement to the opposite direction on actin cables. A recent biochemical study has suggested the processivity of myosin VI (10). The present study addressed this question by using single molecule imaging (11, 12) and optical trapping nanometry (8, 9, 13) that can directly determine the motor processivity at a single molecule level.

MATERIALS AND METHODS

Proteins. Actin was obtained from rabbit skeletal muscle and purified as described (14). Recombinant calmodulin from Xenopus oocytes was cloned and expressed in Sf9 cells as described (15). M5HMM was prepared as described (16). GFP moiety was attached to the N-terminus of M5HMM.

Generation of the expression vectors for myosin VI constructs. A baculovirus transfer vector for mouse myosin VI variants in pFastBac (Gibco-BRL, NY) was produced as follows. Dr. K Avraham (Tel Aviv University) kindly supplied mouse myosin VI cDNA clones containing fragments 150–2565 (B10), 1460–3708 (B2), and 2939–4606 (B12) in pBluescript. A 1679–3309 cDNA fragment of myosin VI was obtained from the B2 clone by Kpn1/PflM1 digestion and was inserted into the B10 clone following its digestion by Kpn1/PflM1. A unique *Nhe*1 site was created at the 5′ side of the initiation codon, and then the myosin VI cDNA was cut by *Nhe*1/*Kpn*1 digestion and inserted into the pFastBac baculovirus transfer vector at the

[1] To whom correspondence and request for materials may be addressed.

0006-291X/02 $35.00

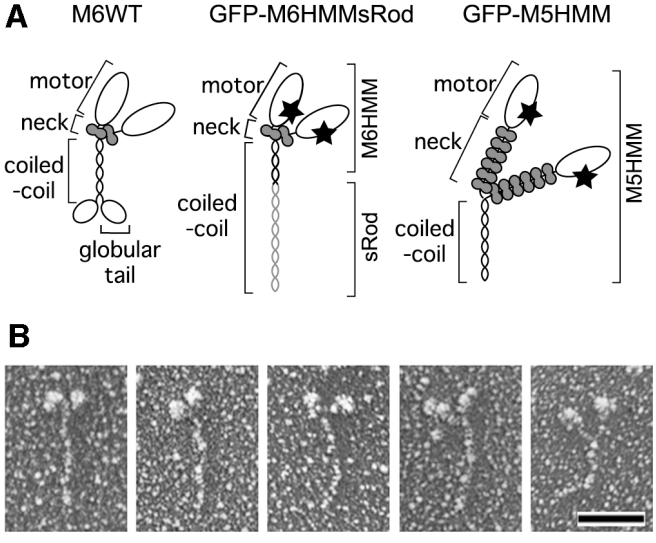

FIG. 1. Structures of the myosin constructs. (A) Schematic representation of M6WT (left), GFP-M6HMMsRod (middle), and GFP-M5HMM (right). GFP moieties were attached to the N-termini of M6HMMsRod and M5HMM. GFP and calmodulin light chain are represented by stars and half tone, respectively. (B) Rotary-shadowed electron microscopic images of GFP-M6HMMsRods. The small globular domain protruded from the head domain is assumed to be a GFP moiety. Scale bar, 50 nm.

polylinker region (M6L). A *Kpn*1 site was created at the 5′ side of the stop codon of B12, and a cDNA fragment (3309–3950) was excised by *Kpn*1 digestion. The fragment was ligated into M6L construct at the *Kpn*1 site. A hexa-histidine tag sequence with a stop codon was introduced at the 3′ side of the *Kpn*1 site. This construct (M6WT), containing the entire coding region, was used to express wild-type myosin VI. To introduce GFP into myosin VI, pEGFP vector (Clontech) was digested with *Nhe*1/*Xba*1 to excise GFP encoding nucleotides. The cDNA fragment was in frame ligated into M6L construct at the unique *Nhe*1 site. A *Spe*1 site was created at nucleotide 3073 of myosin VI cDNA and *Spe*1/*Kpn*1 fragment of smooth myosin II heavy chain cDNA (3325–4699) encoding a part of the coiled-coil domain was introduced into GFPM6L construct to produce GFPM6HMMsRod.

Electron microscopy. Negative-staining was carried out as described (17) with some modifications. A drop of 1.2 μM F-actin solution in a phosphate buffer (5 mM potassium phosphate, pH 8.1, 30 mM KCl, 2 mM $MgCl_2$, 1 mM DTT) was placed on a copper grid. This was rinsed with a few drops of the buffer, followed by a drop of the same buffer containing 0.10–15 μM of GFPM6HMMsRod. After 1 min of incubation, the same buffer but with ~0.2 mM ATP was added. Within 2 to 3 s, it was fixed and stained negatively with a solution of 1% uranyl acetate containing 20 μg/ml bacitracin. The specimens were dried and observed under a JEOL 2000 EX electron microscope. Electron micrographs were taken usually as stereo-pair with 50,000 × to 80,000 × direct magnification. Low angle rotary-shadowing was done according to a standard technique with 6 degrees elevation angle.

Single-motor motility assays. Movements of single fluorescently-labeled myosin molecules were observed as previously described (7, 11, 12) with some modification. The fluorescently-labeled actin filaments, containing biotinylated G-actin (0.5% of total G-actin), were adsorbed onto a quartz surface that had been coated with avidin-biotinylated-casein. The glass surface was then coated with casein to avoid nonspecific binding of myosin. Then, GFP-M6HMMsRod and GFP-M5HMM in the buffer solution containing 25 mM KCl, 5 mM

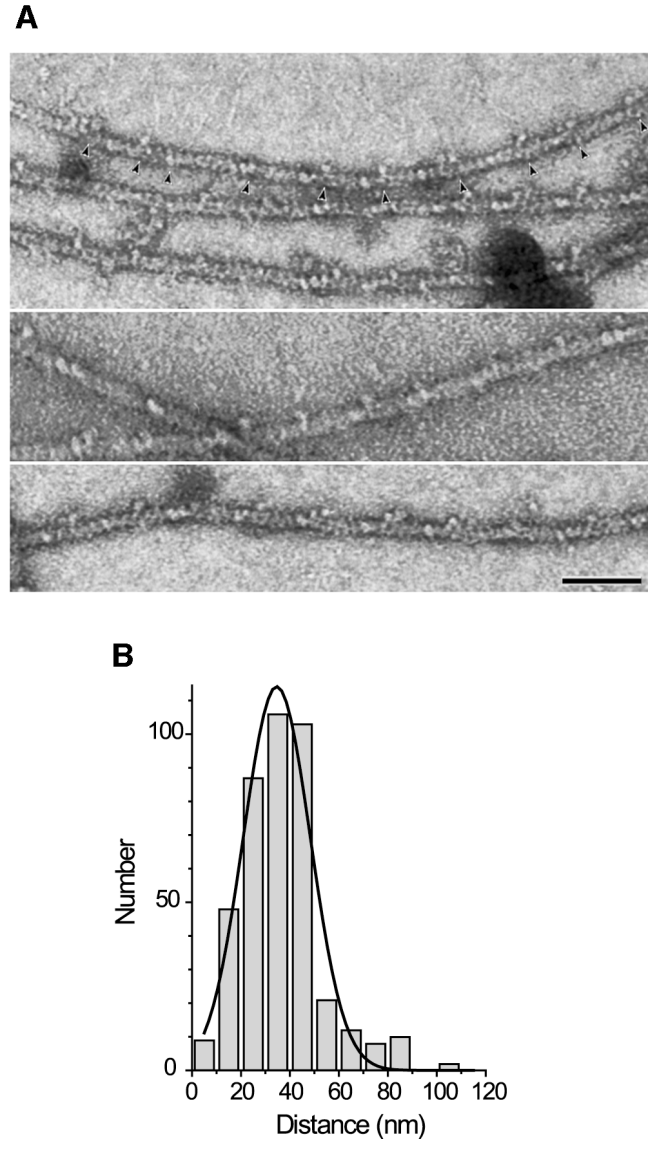

FIG. 2. GFP-M6HMMsRod-actin filament complexes. (A) Negatively-stained electron micrographs. Myosin interacted with actin filaments floating free in the assay buffer containing 0.2 mM ATP. Then the buffer was suddenly replaced with a staining solution to instantaneously arrest the reaction (17). It was confirmed that GFP-M6HMMsRod moves processively along actin filaments with ~36 nm steps at 0.2 mM ATP (Nanometry), although the velocity was several-fold slower than at 5 mM ATP. Arrowheads indicate the positions of GFP-M6HMMsRod molecules bound to actin filaments. Note that the present negative staining method does not use any supporting films, so GFP-M6HMMsRod molecules are kept free in solution until the moment of fixation (17). Scale bar, 50 nm. (B) A histogram of the distance between the two adjacent GFP-M6HMMsRod molecules bound to actin filaments. Some myosin molecules appeared bound to actin filaments with the both heads that are apart with 10–15 nm between them. This may show that myosin molecules switch their track from one to the other protofilament of an actin filament while they slide processively over the actin helical pitch (see Discussion). In such a case, we measured the distance from position of heads at either side to the adjacent myosin molecule on actin (see arrowheads in A). A solid line is a gaussian fit to the data. The mean +/− SD was 35 +/− 14 nm (n = 407).

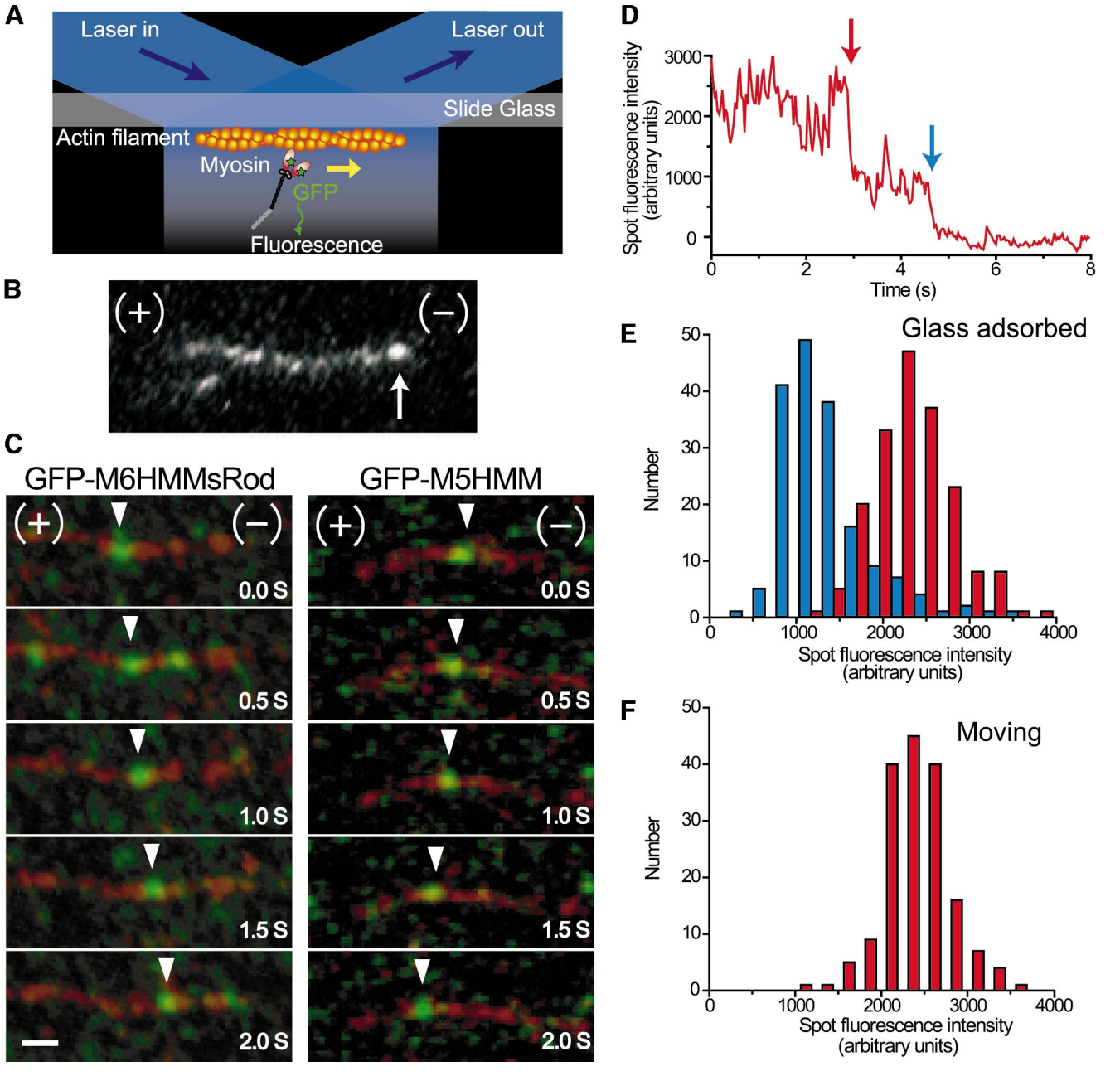

FIG. 3. Processive movement of single molecules of myosin VI and V along actin filaments. (A) Schematic diagram used to observe movement of single myosin molecules by TIRFM. (B) Fluoresce image of a polarity-marked actin filament attached onto a glass surface via biotin-avidin system. A bright spot indicates the bright cap at the pointed end (see Materials and Methods). (C) Sequential images of a single GFP-M6HMMsRod molecule (left panels) and a single GFP-M5HMM molecule (right panels) moving along an actin filament. Fluorescence images of a GFP-M6HMMsRod and an actin filament obtained by dual-view TIRFM were superimposed. (+) and (–) indicate the barbed and pointed ends of actin filaments, respectively. GFP (green) and actin filaments (dark red) were artificially colored. Arrowheads indicate the positions of myosin. Scale bar, 1 μm. (D) A typical time course of photobleaching of a GFP-M6HMMsRod adsorbed onto a glass surface. Photobleaching took place by two steps (marked by arrows). (E) Histograms of fluorescence intensities of GFP-M6HMMsRods measured just after encountering with a glass surface, i.e., before photobeaching (Red-bars) and after the first photobleaching step (Blue-bars). (F) A histogram of fluorescence intensities of GFP-M6HMMsRods moving along an actin filament. The fluorescence intensities of GFP-M6HMMsRods were measured just after encountering with actin filaments, i.e., before photobleaching.

$MgCl_2$, 5 mM ATP, 20 mM Hepes-KOH pH 7.8, 1 mM EGTA, and oxygen scavenger system (14) was added to the actin filament-coated surface. In these experiments, myosin concentrations of ~10 nM were chosen so that individual molecules could be observed on an actin filament without overlap. Polarity-marked actin filaments were prepared as described previously (6, 16) except for labeling actin filaments with only tetramethylrhodamine (TMR). The polarity of the resulting actin filaments were visualized by dimly red through-

out and a highly bright red cap at the pointed end. All experiments were done at 25°C. Optical trapping nanometry was performed as previously described (13) with some modifications. Beads of 0.2 μm in diameter, coated with M6WT and then with bovine serum albumin (BSA), were optically trapped and brought into contact with an actin filaments bound to a glass surface as shown above. Optics: GFP-labeled myosin and TMR-labeled actin filaments were observed by TIRFM (11, 12). GFP and TMR were excited by an Ar-Kr laser (λ = 476.5 nm). Fluorescent images of the two dyes were simultaneously obtained by dual-view optics (18), in which we used a dichroic mirror (Separation WL, 550 nm; Sigmakoki, Saitama, Japan), 515DF30 filter (Omega Optical, Brattleboro, VT) for GFP, 570DF30 filter (Omega) for TMR. The fluorescences were imaged by an EBCCD camera (C-7190-21; Hamamatsu Photonics, Hamamatsu, Japan) coupled with an image intensifier (VS4-1845, Video Scope International, Sterling, VA) and recorded using a digital video recorder. Image analysis: Image analysis was performed on a Macintosh computer using the public-domain program NIHimage with a custom macro. Fluorescent intensities were obtained using a rolling 4-frame average to reduce the fluctuations, by summing the intensities from an 7 $\times$ 7 pixel window and subtracting the background intensity. Positions of single myosin molecules were measured from the centroids of the fluorescent spots. Standard deviations of the myosins rigidly attached to the glass surface were 60 nm, which correspond to the space resolution.

ATPase assay and in vitro motility assay. The steady-state ATPase activity was determined at 25°C as described using the ATP regeneration system (19). The surface gliding assay was performed as described previously (16). Actin filament velocity was calculated from the movement distance and the elapsed time in successive snapshots. Student's *t* test was used for the statistical comparison of mean values. A value of $P < 0.01$ was considered to be significant.

RESULTS AND DISCUSSION

We constructed chimeric myosin VI (GFP-M6HMMsRod) (Fig. 1A middle). It contained the motor domain, neck domain, and entire coiled–coil of myosin VI. To stabilize the formation of the two-headed structure and visualize by fluorescence microscopy, additional short coiled–coil domain (sRod) of myosin II that is too short to form filaments (20) and GFP (green fluorescent protein) were attached to the C-terminal and N-terminal ends of the construct, respectively. GFP-M6HMMsRod as well as wild-type myosin VI (M6WT) was coexpressed with calmodulin in Sf9 insect cells. Electron microscopy revealed that GFP-M6HMMsRod had two heads connected with an extended rod as expected from the designed construct (Figs. 1B and 2A). GFP-M5HMM was also constructed for comparison (Fig. 1A right). The actin-activated ATPase activity (3 head^{-1} s^{-1}) of the GFP-M6HMMsRod was identical to M6HMM. The actin translocating velocity of GFP-M6HMMsRod (300 nms^{-1}) in the surface gliding assay was identical to that of M6HMM and M6WT. Thus, N-terminal GFP moiety neither influenced the actin-activated ATPase activity nor the actin translocating velocity.

The movements of GFP-M6HMMsRods on actin filaments were directly observed using TIRFM (7, 11, 12) (Fig. 3A). GFP-M6HMMsRods could be observed binding to and moving along actin filaments (Fig. 3C, left panels). The direction of movement was checked by

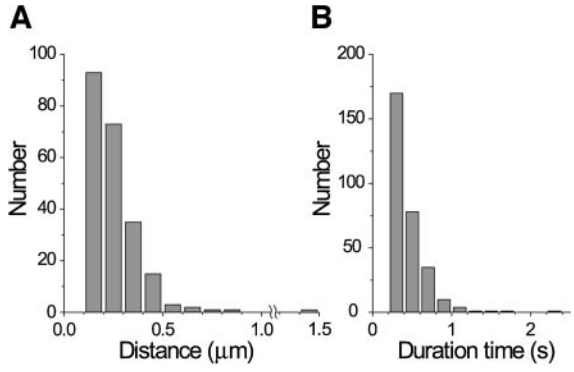

FIG. 4. Histograms of travel distances (A) and durations (B) of GFP-M6HMMsRods moving along actin filaments.

polarity-marked actin filaments (6, 16) (Fig. 3B). The direction of GFP-M6HMMsRod movement was consistent with the previous report for myosin VI subfragment-1 (6) but opposite to that of GFP-M5HMM (Fig. 3C, right panels). To verify that moving fluorescent spots were indeed due to single GFP-M6HMMsRod molecules, the photobleaching characteristics and intensities of fluorescent spots were examined (12). The fluorescent spots of surface-adsorbed GFP-M6HMMsRods disappeared primarily in a two-step process, as expected for photobleaching reactions of two GFP molecules bound to the GFP-M6HMMsRod (Fig. 3D). The fluorescence intensity measured just after binding to the glass surface, i.e., before photobleaching (Fig. 3E, Red-bars) was approximately twice as large as that after the first photobleaching step (Fig. 3E, Blue-bars). The fluorescence intensity of moving spots (Fig. 3F), which was measured just after encountering the actin filaments, was similar to that of adsorbed ones before photobleaching. These results indicate that moving spots were due to single GFP-M6HMMsRod molecules.

Figures 4A and 4B show the travel distance and duration of attachment of single GFP-M6HMMsRod molecules, respectively. The mean travel distance and duration were 240 nm and 0.44 s, respectively. The travel distance (240 nm) is consistent with a recent biochemical result that the number of ATP molecules per encounter with actin is ~5 (10), if one ATP molecule is assumed to be hydrolyzed per 36 nm step (9). About 60% of GFP-M6HMMsRods encountering with the actin filament moved more than 100 nm, which was the distance that could be sufficiently determined by the computer image analysis (see Materials and Methods). The mean velocity calculated from these values is 550 nm/s (=240 nm/0.44 s), which is larger than the gliding velocity of actin filaments on GFP-M6HMMsRod- and M6WT-coated glass surfaces (~300 nm/s). A similar difference was observed for fluorescently-labeled wild-type myosinV (7). This is probably because in the surface gliding assay, many myosins interact with an actin filament that provides internal friction.

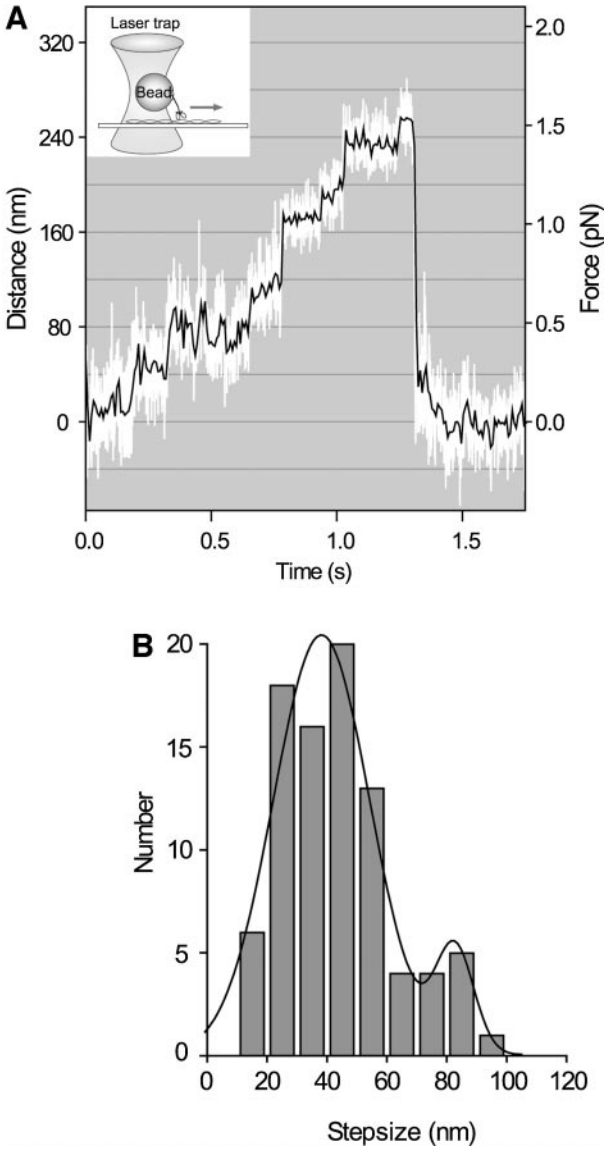

FIG. 5. Optical trapping nanometry of bead-tagged M6WT moving along actin filaments. (A) A typical record of the time course of motion of an optically trapped bead coated with M6WT along an actin filament. White dots, raw data. Black line, same data passed through a low-pass filter of 50 Hz bandwidth. Right ordinate indicates force calculated as (displacement) × (trap stiffness). Trap stiffness, 0.005–0.01 pN/nm. (B) A histogram of the step size. Data were fit to two gaussians with peaks at 38 nm (SD = 16 nm) and at 82 nm (SD = 6 nm). A small gaussian at 82 nm may be due to two successive steps taking place rapidly within the temporal resolution (2 ms) of the measurement system.

To spy on the process of processive movement of myosinVI, we measured the movement of an optically-trapped bead coated with M6WT. An optically-trapped M6WT-coated bead was brought into contact with an actin filament adsorbed on a glass surface. The movement of M6WT was determined by measuring the displacement of a bead with nanometer accuracy (13) (Fig. 5A, insertion). The displacement took place processively in a stepwise fashion, reached a plateau and fell suddenly to zero displacement (Fig. 5A). We confirmed by Poisson statistics that single myosin VI molecules are sufficient to move beads (9). The number of beads moving continuously (>100 nm) along actin filaments was recorded as a function of the molar ratio of myosin VI molecules to beads. The probability that a bead carries one or more motors is $(1 - \exp(-\lambda c))$, where c is the molar ratio of myosin VI molecules to beads during the incubation and λ is a fit parameter accounting for the fact that not all myosin VI molecules incubated together with the beads will find a bead or adsorb in a functional conformation (8, 9). The data could be well fit by this functional form ($\lambda = 0.01$, reduced $\chi^2 = 0.04$), showing that a single molecule is sufficient to move a bead. The experiments were performed at the myosin VI to bead ratio where <30% of the beads were moving. Assuming a myosin VI has 100 nm of reach, >94% of moving beads should be driven by only one molecule. The stall force (1.5–2.0 pN) was constant, agreeing that the number of M6WT molecules involved in the movement at a time is one. Figure 4B shows a histogram of stepsize. The average stepsize was ~38 nm. A small peak around 80 nm is probably due to two successive steps taking place rapidly within the temporal resolution (2 ms) of the measurement system. When the concentration of ATP was decreased from 5 mM to 75 μM, the dwell time was longer but the stepsize was unchanged. This result excludes the possibility that ~38 nm steps are composed of small steps, each of which is coupled to the ATPase cycle, but they could not be observed due to lack of the temporal resolution.

How does myosin VI with a short neck domain processively move along the actin filament with large (38 nm) steps? It is proposed that myosin V with a long (23 nm) neck domain strides along the helical repeat of an actin filament by tilting the long neck domain of one head and leading the partner head to the neighbor helical pitch (36 nm) (9, 23), based on the lever arm model (21, 22). Therefore, one possibility is that the α-helix coiled–coil connecting the two heads at the far ends of their neck domains (Fig. 1A) unzips so that the heads can span the actin helical pitch. In rotary-shadowed electron micrographs of GFP-M6HMMsRods, some molecules appeared unzipping at the coiled–coil domain, though the majority of the molecules were not unzipped (Fig. 1B). The result suggests that there is flexibility near the neck domain. However, it is unlikely that the possible unzipping enables myosin VI to step the helical pitch of actin. First, negatively stained images of electron micrographs did not show unzipping of myosin VI thus spanning the helical pitch of actin filaments. A GFP-M6HMMsRod molecule bound to the actin monomer with ~36 nm intervals corresponding to the actin helical pitch (Fig. 2A). Second, even if myosin VI coiled–coil is unzipped, such a flexible structure is unlikely to produce force and actually the

"lever-arm" model of the cross-bridge movement requires a rigid structure of "lever-arm" domain. The elastic modulus of a single α-helix for bending is estimated to be 0.0015 pN/nm(24), if the length is 23 nm. If the neck domain tilts the α-helix so that its far end is swung by 36 nm, the force generated at the far end would be only 0.054 pN (=0.0015 pN/nm $\times$ 36 nm). By this mechanism, myosin VI cannot move with 36 nm steps at >0.05 pN (Fig. 5A).

Figure 2A shows a negatively-stained images of GFP-M6HMMsRod-actin filament complexes in the presence of 0.2 mM ATP. Interestingly, GFP-M6HMMsRod molecules bound to an actin filament with 35 +/− 14 nm (mean +/− SD, n = 407. Fig. 2B) intervals, coinciding with the actin helical pitch. This result suggests that GFP-M6HMMsRod molecules cooperatively bind to an actin filament, i.e., when a myosin head binds to some position of an actin filament, the other head preferentially binds to the position ~36 nm (one helical pitch) apart from the prebound head. Recently, it was found by negative-stain electron microscopy that mutant *Dictyostelium* myosin II subfragment −1 (one head), in which the 680th Gly is replaced by Val so that it forms a long-life actomyosin complex in the presence of ATP like myosin VI, periodically binds along one side of an actin filament at 36 nm intervals in the presence of ATP (E. Katayama and T. Q. P. Uyeda, unpublished data). Based on these findings, we propose a model that the binding of a head of myosin VI evokes a "hot spot" on the actin filament at 36 nm (actin helical pitch) apart from the initial binding site due to the conformational changes in an actin filament upon myosin binding. The partner head slides to the 'hot spot' thus producing the 36 nm step. This process occurs successively thus yielding a processive movement. We have recently demonstrated that the replacement of the neck domain and converter domain of myosin V (a plus directed myosin) by those of myosin VI (a minus directed myosin) does not affect the directionality, indicating that the directionality is solely determined by the motor core domain of myosin but not converter/lever-arm domain (16). The direction of the movement to the neighboring "hot spot" would be determined by the myosin isotype specific interaction at the interface between myosin head and actin that creates a bias on the Brownian motion.

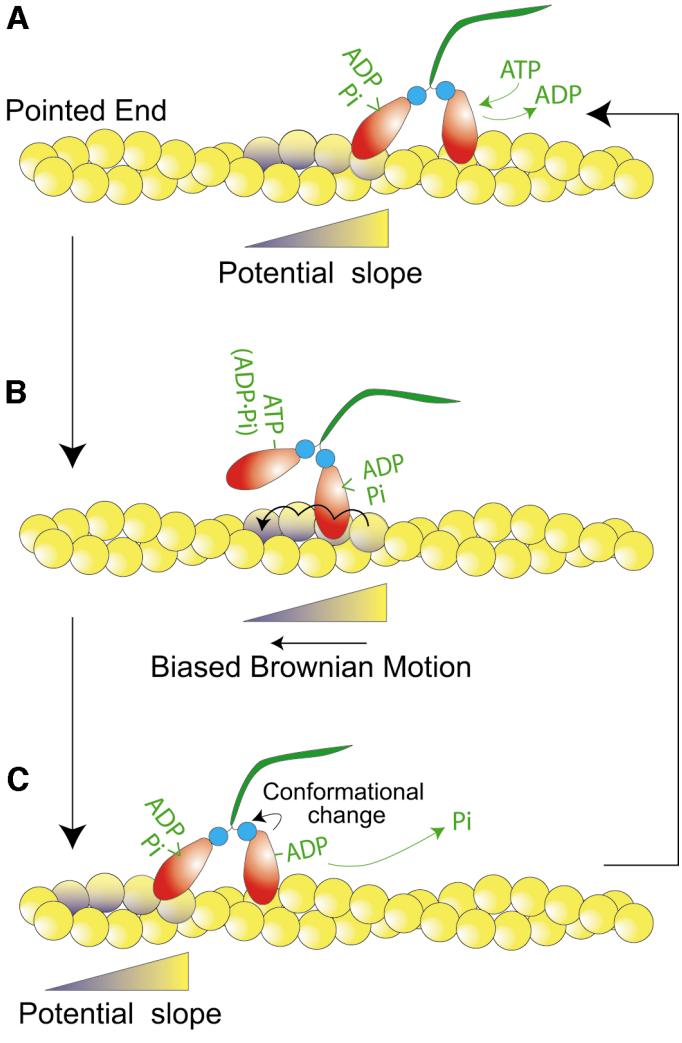

FIG. 6. Model of myosin VI stepping. The binding of a myosin head causes partial untwisting of the actin filament thus exposing the hydrophobic region (purple) between protofilaments and producing a potential slope (A). The partner head is led to the next helical pitch and moves along the potential slope by biased Brownian Motion (B). When the head reaches the potential minimum, Pi is released from the head, followed by conformational changes in the neck domain, and then the head stops the movement. At that time, the potential slope is produced at the next helical pitch (C). State (C) is the rate limiting state, so the conformation of myosin VI in the state (C) is prominent in the electron micrograph. This model is based on our electron microscopic observations and Katayama and Uyeda (see text).

Myosin VI may rapidly walk along the actin monomer repeat to produce a large step. We have recently suggested that a myosin II head walks along the actin monomer repeat by biased Brownian motion (14, 25). A potential slope made along the helical pitch of an actin filament upon myosin binding may bias the Brownian motion of myosin VI (Fig. 6). While how such a potential slope along the helical pitch could be produced is obscure, there are a number of reports suggesting that conformational changes in actin filaments are involved in actomyosin force generation (26–30). When actin filaments are chemically cross-linked and its motions are suppressed, the actin-activated ATPase activity of myosin is little affected but the motility is lost (26, 27). Long-range conformational changes along actin filaments are suggested (26, 28, 29). An x-ray diffraction study has indicated that actin filaments are untwisted during force generation in muscle (30). It is plausible that the binding of myosin head causes partial untwisting of actin helix thus exposing the hydrophobic region between the protofilaments and producing a potential slope.

In summary, the neck domain length is critical to neither the processivity nor large step of myosin. Conformational changes in actin filaments upon the binding of myosin may play an important role in the processive and large steps of myosin VI.

(A paper showing the processive movement of myosin VI with a large step (31) was published just before we submitted this paper.)

ACKNOWLEDGMENTS

We thank H. Tanaka, K. Kitamura, and M. Nishiyama (Single molecule process project) and T. Q. P. Uyeda for their technical advice.

REFERENCES

1. Hodge, T., and Cope, M. J. (2000) A myosin family tree. *J. Cell Sci.* **113,** 3353–3354.
2. Cheney, R. E., O'Shea, M. K., Heuser, J. E., Coelho, M. V., Wolenski, J. S., Espreafico, E. M., Forscher, P., Larson, R. E., and Mooseker, M. S. (1993) Brain myosin-V is a two-headed unconventional myosin with motor activity. *Cell* **75,** 13–23.
3. Mermall, V., McNally, J. G., and Miller, K. G. (1994) Transport of cytoplasmic particle catalyzed by an unconventional myosin in living *Drosophila* embryo. *Nature* **369,** 560–562.
4. Buss, F., Kendrick-Jones, J., Lionne, C., Knight, A. E., Cote, G. P., and Paul Luzio, J. (1998) The localization of myosin VI at the golgi complex and leading edge of fibroblasts and its phosphorylation and recruitment into membrane ruffles of A431 cells after growth factor stimulation. *J. Cell Biol.* **143,** 1535–1545.
5. Kelleher, J. F., Mandell, M. A, Moulder, G., Hill, K. L., L'Hernault, S. W., Barstead, R., and Titus, M. A. (2000). Myosin VI is required for asymmetric segregation of cellular components during *C. elegans* spermatogenesis. *Curr. Biol.* **10,** 1489–1496.
6. Wells, A. L., Lin, A. W., Chen, L. Q., Safer, D., Cain, S. M., Hasson, T., Carragher, B. O., Milligan, R. A., and Sweeney, H. L. (1999) Myosin VI is an actin-based motor that moves backwards. *Nature* **401,** 505–508.
7. Sakamoto, T., Amitani, I., Yokota, E., and Ando, T. (2000) Direct observation of processive movement by individual myosin V molecules. *Biochem. Biophys. Res. Commun.* **272,** 586–590.
8. Mehta, A. D., Rock, R. S., Rief, M., Spudich, J. A., Mooseker, M. S., and Cheney, R. E. (1999) Myosin-V is a processive actin-based motor. *Nature* **400,** 590–593.
9. Rief, M., Rock, R. S., Mehta, A. D., Mooseker, M. S., Cheney, R. E., and Spudich, J. A. (2000) Myosin-V stepping kinetics: A molecular model for processivity. *Proc. Natl. Acad. Sci. USA* **97,** 9482–9486.
10. De La Cruz, E. M., Ostap, E. M., and Sweeney, H. L. (2001) Kinetic mechanism and regulation of myosin VI. *J. Biol. Chem.* **276,** 32373–32381.
11. Funatsu, T., Harada, Y., Tokunaga, M., Saito, K., and Yanagida, T. (1995) Imaging of single fluorescent molecules and individual ATP turnovers by single myosin molecules in aqueous solution. *Nature* **374,** 555–559.
12. Vale, R. D., Funatsu, T., Pierce, D. W., Romberg, L., Harada, Y., and Yanagida, T. (1996) Direct observation of single kinesin molecules moving along microtubules. *Nature* **380,** 451–453.
13. Nishiyama, M., Muto, E., Inoue, Y., Yanagida, T., and Higuchi, H. (2001) Substeps within the 8-nm step of the ATPase cycle of single kinesin molecules. *Nature Cell Biology* **3,** 425–428.
14. Kitamura, K., Tokunaga, M., Iwane, A. H., and Yanagida, T. (1999) A single myosin head moves along an actin filament with regular steps of 5.3 nanometers. *Nature* **397,** 129–134.
15. Ikebe, M., Kambara, T., Stafford, W. F., Sata, M., Katayama, E., and Ikebe, R. (1998) A hinge at the central helix of the regulatory light chain of myosin is critical for phosphorylation-dependent regulation of smooth muscle myosin motor activity. *J. Biol. Chem.* **273,** 17702–17707.
16. Homma, K., Yoshimura, M., Saito, J., Ikebe, R., and Ikebe, M. (2001) The core of the motor domain, not the lever-arm/converter domain, determines the direction of myosin movement. *Nature* **412,** 831–834.
17. Katayama, E. (1989) The effects of various nucleotides on the structure of actin-attached myosin subfragment-1 studied by quick-freeze deep-etch electron microscopy. *J. Biochem.* **106,** 751–770.
18. Kinosita, K., Jr., Itoh, H., Ishiwata, S., Hirano, K., Nishizaka, T., and Hayakawa, T. (1991) Dual-view microscopy with a single camera: Real-time imaging of molecular orientations and calcium. *J. Cell Biol.* **115,** 67–73.
19. Homma, K., Saito, J., Ikebe, R., and Ikebe, M. (2001) Motor function and regulation of myosin X. *J. Biol. Chem.* **276,** 34348–34354.
20. Ikebe, M., Komatsu, S., Woodhead, J. L., Mabuchi, K., Ikebe, R., Saito, J., Craig, R., and Higashihara, M. (2001) The tip of the coiled–coil rod determines the filament formation of smooth muscle and non-muscle myosin. *J. Biol. Chem.* **276,** 30293–300.
21. Rayment, I., Rypniewski, W. R., Schmidt-Base, K., Smith, R., Tomchick, D. R., Benning, M. M., Winkelmann, D. A., Wesenberg, G., and Holden, H. M. (1993) Three-dimensional structure of myosin subfragment-1: A molecular motor. *Science* **261,** 50–58.
22. Spudich, J. A. (1994) How molecular motors work. *Nature* **372,** 515–518.
23. Walker, M. L., Burgess, S. A., Sellers, J. R., Wang, F., Hammer, J. A. 3rd, Trinick, J., and Knight, P. J. (2000) Two-headed binding of a processive myosin to F-actin. *Nature* **405,** 804–807.
24. Hofmann, H., Voss, T., and Kuhn, K. (1984) Localization of flexible sites in thread-like molecules from electron micrographs. Comparison of interstitial, basement membrane and intima collagens. *J. Mol. Biol.* **172,** 325–343.
25. Yanagida, T., Esaki, S., Iwane, A. H., Inoue, Y., Ishijima, A., Kitamura, K., Tanaka, H., and Tokunaga, M. (2000) Single-motor mechanics and models of the myosin motor. *Phil. Trans. R. Soc. London. B* **355,** 441–447.
26. Prochniewicz, E., and Yanagida, T. (1990) Inhibition of sliding movement of F-actin by crosslinking emphasizes the role of actin structure in the mechanism of motility. *J. Mol. Biol.* **216,** 761–772.
27. Kim, E., Bobkova, E., Miller, C. J., Orlova, A., Hegyi, G., Egelman, E. H., Muhlrad, A., and Reisler, E. (1998) Intrastrand cross-linked actin between Gln-41 and Cys-374. III. Inhibition of motion and force generation with myosin. *Biochem.* **37,** 17801–17809.
28. Egelman, E. H., Francis, N., and DeRosier, D. J. (1982) F-actin is a helix with a random variable twist. *Nature* **298,** 131–135.
29. Schutt, C. E., and Lindberg, U. (1992) Actin as the generator of tension during muscle contraction. *Proc. Acad. Sci. USA* **89,** 19–23.
30. Takezawa, Y., Sugimoto, Y., and Wakabayashi, K. (1998) Extensibility of the actin and myosin filaments in various states of skeletal muscle as studied by X-ray diffraction. *Adv. Exp. Med. Biol.* **453,** 309–16; discussion 317.
31. Rock, R. S., Rice, S. E., Wells, A. L., Purcell, T. J., Spudich, J. A., and Sweeney, H. L. (2001) Myosin VI is a processive motor with a large step size. *Proc. Natl. Acad. Sci. USA* **98,** 3655–13659.